Neuron, Vol. 25, 307–316, February, 2000, Copyright ©2000 by Cell Press

# Essential Roles of *Drosophila* RhoA in the Regulation of Neuroblast Proliferation and Dendritic but Not Axonal Morphogenesis

**Tzumin Lee, Christopher Winter, Simone S. Marticke, Arthur Lee, and Liqun Luo***
Department of Biological Sciences
Stanford University
Stanford, California 94305

## Summary

**The pleiotropic functions of small GTPase Rho present a challenge to its genetic analysis in multicellular organisms. We report here the use of the MARCM (mosaic analysis with a repressible cell marker) system to analyze the function of RhoA in the developing *Drosophila* brain. Clones of cells homozygous for null *RhoA* mutations were specifically labeled in the mushroom body (MB) neurons of mosaic brains. We found that *RhoA* is required for neuroblast (Nb) proliferation but not for neuronal survival. Surprisingly, *RhoA* is not required for MB neurons to establish normal axon projections. However, neurons lacking *RhoA* overextend their dendrites, and expression of activated RhoA causes a reduction of dendritic complexity. Thus, RhoA is an important regulator of dendritic morphogenesis, while distinct mechanisms are used for axonal morphogenesis.**

## Introduction

The small GTPase Rho is highly conserved from yeast to humans. It is implicated in regulating diverse cellular functions, including cell adhesion and motility, cytokinesis, membrane trafficking, transcription activation, cell growth and transformation, and neuronal growth cone signaling (reviewed by Narumiya, 1996; Luo et al., 1997; Van Aelst and D'Souza-Schorey, 1997; Hall, 1998). In particular, mammalian RhoA has been shown to induce cell rounding and process retraction in PC12 cells and in neuroblastoma cells in response to extracellular agonists (Jalink et al., 1994; Kozma et al., 1997; Hirose et al., 1998). However, other studies have suggested that RhoA promotes dendritic and axonal growth in cortical neurons in primary culture (Threadgill et al., 1997). With the exception of yeast, almost all studies have relied on dominant mutants or the C3 exoenzyme toxin to interfere with Rho activity. It is therefore important to test the in vivo function of Rho using loss-of-function mutants in multicellular organisms. Two technical obstacles complicate genetic studies of Rho function in mammals: potential pleiotropic effects of blocking Rho function and possible genetic redundancy between three highly related proteins, RhoA, RhoB, and RhoC (reviewed by Valencia et al., 1991).

The *Rho1/RhoA* gene is the single *Drosophila* ortholog of mammalian RhoA, RhoB, and RhoC (Hariharan et al., 1995; Strutt et al., 1997). *Drosophila* embryos homozygous for null mutations of *RhoA* zygotically arrest development with defects in dorsal closure (Strutt et al., 1997; Lu and Settleman, 1999). It is likely that *RhoA* is required in much earlier developmental stages (Barrett et al., 1997) but that such a requirement is masked by the maternal contribution of *RhoA* mRNA (Hariharan et al., 1995). Analysis of clones homozygous for hypomorphic alleles has revealed a function for RhoA in the establishment of tissue polarity (Strutt et al., 1997). Clones homozygous for null alleles of *RhoA* were undetectable using conventional systems of marking mosaic cells (Xu and Rubin, 1993; Strutt et al., 1997).

To study the in vivo functions of *RhoA* in the developing central nervous system, we made use of the MARCM (mosaic analysis with a repressible cell marker) system (Lee and Luo, 1999) to label *RhoA* mutant neurons, specifically in mosaic flies. We found that RhoA is required for neuroblast (Nb) proliferation but not for neuronal survival. Neurons null for *RhoA* mutations establish normal axonal projections but extend dendrites beyond their normal spatial confines. Conversely, expression of constitutively active RhoA results in a reduction of dendritic volume and complexity. In a separate study, we show that expression of constitutively active RhoA in hippocampal pyramidal neurons in cultured brain slices results in a drastic reduction of dendritic complexity (A. Y. Nakayama et al., submitted). These experiments identify RhoA as an important regulator of dendritic morphogenesis in both *Drosophila* and mammalian neurons.

## Results and Discussion

### Gross Phenotypes of *RhoA* Mutants in Mushroom Body Development

We used the MARCM system to label only homozygous mutant cells in mosaic organisms (Lee and Luo, 1999). In this system, the repressor of the GAL4 transcriptional activator, GAL80, is made from a ubiquitously expressed *tubP-GAL80* transgene on the chromosome in *trans* to the homologous chromosome containing a *RhoA* null mutation ($RhoA^{72O}$ or $RhoA^{72R}$) (Strutt et al., 1997). Both *RhoA* and *tubP-GAL80* are distal to a pair of homologous FRT sites. Mitotic recombination at the FRT sites gives rise to a daughter cell that is homozygous for *RhoA* and lacks *tubP-GAL80*. The absence of GAL80 allows GAL4 to drive the expression of a UAS cell marker in precisely the cells that lack the *RhoA* gene. Using this system, mitotic recombination results in the generation and visualization of three types of clones in the *Drosophila* CNS: Nb, two cell, and single cell clones (Figure 1A).

We focused our study on the mushroom body (MB) neurons of the *Drosophila* brain. A wild-type MB Nb clone generated in a newly hatched larva and examined at the wandering third instar stage (about 100 hr later) (see Experimental Procedures for details) always contains over 150 neurons. These neurons project their dendrites into a region called the calyx and project their

*To whom correspondence should be addressed (e-mail: lluo@stanford.edu).

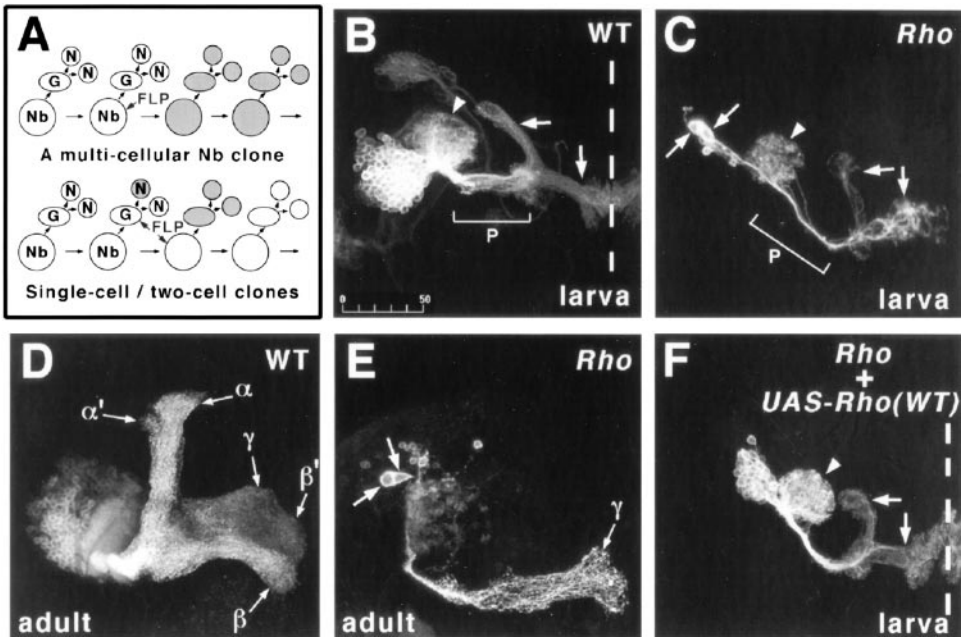


Figure 1. Gross Phenotypes of *RhoA* Nb Clones in MBs

(A) In the *Drosophila* CNS, a Nb undergoes asymmetric division to regenerate another Nb and a ganglion mother cell (G), which undergoes one more division to give rise to two postmitotic neurons (N). In the MARCM system (Lee and Luo, 1999), loss of the repressor transgene in the Nb after mitotic recombination leads to the formation of a multicellular Nb clone that contains the rest of the lineage (top). Loss of the repressor gene in the ganglion mother cell or during the only division of the ganglion mother cell gives rise to a two cell or a single cell clone, respectively (bottom).

(B and C) In wandering third instar larvae, a wild-type MB Nb clone (B) contains more than 150 neurons, whereas a *RhoA* mutant Nb clone (C) contains 10–12 nuclei, including two large nuclei (oblique arrows). Arrowheads point to dendrites projecting into the calyx. Vertical and horizontal arrows point to the axons projecting into the medial and vertical lobes, respectively. Brackets indicate the peduncle.

(D and E) In an adult wild-type Nb clone, three types of MB neurons send their axons into five distinct lobes (D) (Lee et al., 1999), whereas an adult *RhoA* Nb clone contains 10–12 cells, including two large nuclei (arrows), that extend their axons only to the $\gamma$ lobe (E).

(F) Expression of *UAS-RhoA(wt)* in a *RhoA* MB Nb clone largely rescues the *RhoA* phenotype, as evidenced by more cells, lack of large nuclei, and denser calyx (arrowhead) and lobes (arrows) compared with (C).

All images are composite confocal images of either anti-mCD8 immunostaining (B, C and F) or GFP fluorescence (D and E). The panneuronal *GAL4-C155* is used to visualize all postmitotic neurons devoid of the GAL80 repressor (Lee and Luo, 1999). The right side of the brain, mounted in an oblique fashion, is shown in this and all of the following figures, such that dorsal-anterior is at the top. Midline is to the right of the image, as shown by the dotted line in (B) and (F).

The units in this and all following scale bars are micrometers. Genotypes: *GAL4-C155*,*hs-FLP/Y*; $FRT^{G13}$,*UAS-mCD8-GFP*/$FRT^{G13}$,*tubP-GAL80* (B and D); *GAL4-C155*,*hs-FLP/Y*; $FRT^{G13}$,*UAS-mCD8-GFP*, $RhoA^{72R}$/$FRT^{G13}$,*tubP-GAL80* (C and E); and *GAL4-C155*,*hs-FLP/Y*; $FRT^{G13}$,*UAS-mCD8-GFP*, $RhoA^{72R}$/$FRT^{G13}$,*tubP-GAL80*; *UAS-RhoA(wt)*/+ (F).

axons through the peduncle, into the medial and vertical lobes (Lee and Luo, 1999; Lee et al., 1999) (Figure 1B). MB Nb clones homozygous for *RhoA* null mutations consistently contained about 10–12 cells (hereafter referred to as *RhoA* cells or neurons); within each clone, two of these nuclei (identified as unstained centers, outlined by the mCD8-GFP signal; see below) were much larger than the rest of the nuclei (Figure 1C). When examined in adulthood, wild-type Nb clones contained over 500 neurons that projected axons to five lobes (Crittenden et al., 1998; Lee et al., 1999) (Figure 1D), whereas *RhoA* Nb clones still contained about 10–12 cells with axons projecting to only one medial lobe (Figure 1E). Expression of a *UAS-RhoA(wt)* transgene specifically in *RhoA* mutant Nb clones partially rescued the phenotype (Figure 1F), indicating that the observed defect was a result of loss of RhoA function. The rescue was not complete, perhaps due to the late onset of GAL4-induced transgene expression resulting from the perdurance of the GAL80 repressor protein, weak expression of *GAL4-C155* in MB Nbs, or both.

### *RhoA* Is Required for Nb Proliferation

Several lines of evidence indicate that the reduced *RhoA* Nb clone size is caused by an arrest of Nb proliferation, rather than neuronal death. First, bromodeoxyuridine (BrdU) pulse-labeling experiments at different stages of development indicated that *RhoA* MB Nbs ceased division within 24 hr after clone induction. In these experiments, Nb clones were generated in newly hatched larvae by heat shock induction of FLP recombinase from a hs-FLP transgene, and larvae were exposed to BrdU at different times afterward (see Experimental Procedures). Clones were examined at either 36 hr post heat shock in second instar larvae (Figures 2A–2D) or over 100 hr later in wandering third instar larvae (data not shown), with similar results in both cases. When larvae were exposed to BrdU 3–12 hr after heat shock, BrdU was incorporated into most small *RhoA* nuclei (Figure 2A), while a BrdU pulse at 12–18 hr resulted in incorporation in two to four small and two large *RhoA* nuclei (Figure 2B). A BrdU pulse at 18–24 hr post heat shock always resulted in exclusive labeling of the two large

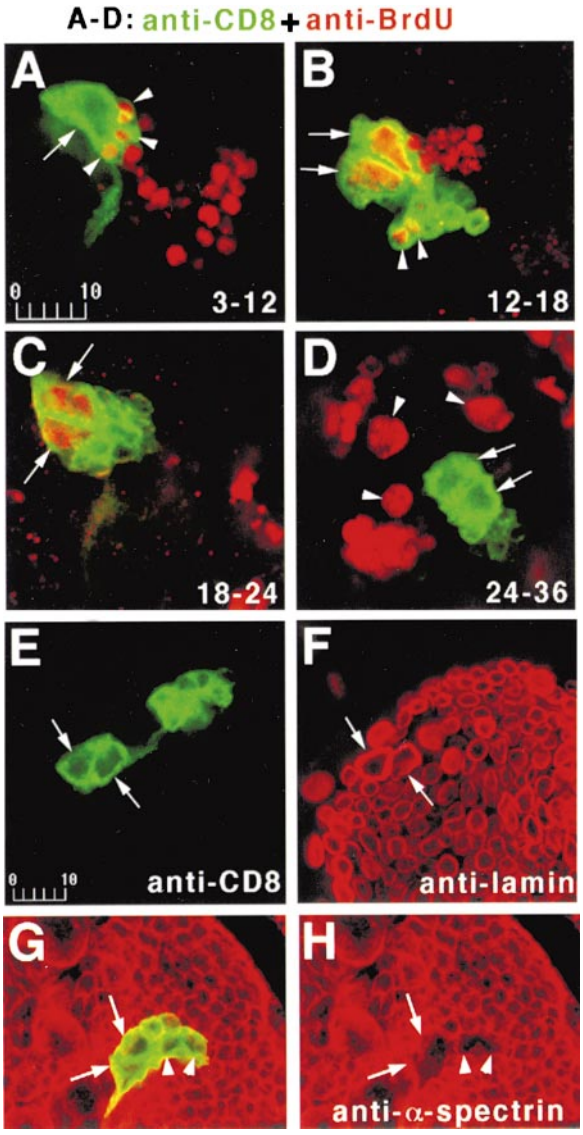


Figure 2. Requirement of *RhoA* for MB Nb Proliferation

All images represent single confocal sections double labeled in green for mCD8 to mark the clones and in red for anti-BrdU (A to D), anti-lamin (F), or anti-α-spectrin (G and H). Not all cells in *RhoA* clones are in the focal plane.

(A–D) Time course of BrdU pulse labeling (hours post heat shock induction of mitotic recombination are shown) revealed birth time of *RhoA* mutant cells. Arrows in (A) through (D) point to large *RhoA* nuclei. Arrowheads in (A) and (B) point to the normal size BrdU-labeled *RhoA* nuclei. Arrowheads in (D) point to three neighboring wild-type MB Nbs still incorporating BrdU.

(E and F) mCD8-GFP staining (E) outlined the nuclei, as confirmed by the immunostaining for lamin, a nuclear membrane marker (F). Note both large nuclei in a *RhoA* Nb clone (arrows) are clearly outlined by immunostaining for either mCD8 (E) or lamin (F).

(G and H) Marking the plasma membrane specifically with anti-α-spectrin antibody (red) revealed some cell bodies containing two nuclei in a *RhoA* Nb clone (green), consistent with a cytokinesis defect. The two large nuclei (arrows) are always together in one cell body. Some small nuclei also exist as two nuclei within a cell body (arrowheads).

Heat shock was performed in newly hatched larvae, and at least eight clones from each manipulation were examined 36 hr later with consistent results. A MB GAL4 line, *GAL4-201Y*, was used to facilitate the visualization of MB neurons. *GAL4-201Y* is located on chromosome arm 2R, and hence in homozygous *RhoA* cells the GAL4 transgene is doubled.

Genotype: *hs-FLP/X* or *-Y*; $FRT^{G13}$,*UAS-mCD8-GFP*, $RhoA^{72O}$,*GAL4-201Y*/$FRT^{G13}$,*tubP-GAL80*.

nuclei (Figure 2C). BrdU pulses at 24–36 hr (Figure 2D) or thereafter (data not shown) failed to label *RhoA* cells, whereas marked wild-type MB Nb clones incorporated BrdU at all times tested (data not shown). Second, we generated *RhoA* MB Nb clones at different developmental stages and analyzed them in adults. We invariably observed an arrest of Nb proliferation with Nb clones containing 10–20 cells with two large nuclei (data not shown), indicating that the requirement for RhoA in Nb proliferation is not stage specific. Last, when *RhoA* clones were generated in newly hatched larvae, the 10–12 *RhoA* cells could be observed as early as 36 hr after clone induction (Figures 2A–2E) and as late as in 10-day-old adult (Figure 1E). Thus, RhoA is not required for the long-term survival of MB neurons, supporting the alternative view, that RhoA is needed to generate neurons.

### *RhoA* Mutant Nbs Are Arrested in Cytokinesis

Rho has previously been shown to regulate cytokinesis (Kishi et al., 1993; Mabuchi et al., 1993) and G1/S transition (Yamamoto et al., 1993; Olson et al., 1995), both of which are essential for normal cell proliferation. To test whether *RhoA* Nb clones arrest proliferation at G1/S transition, we mapped more precisely the birth time of *RhoA* mutant cells. Because of the perdurance of the GAL80 protein (Lee and Luo, 1999), we were not able to identify clones reliably using the expression of mCD8-GFP until 24 hr after heat shock induction of mitotic recombination. However, *RhoA* Nb clones were readily identifiable based on the presence of two adjacent large nuclei using nuclear lamin staining (Smith and Fisher, 1989) (Figure 2F), and the MB region was identified based on its unique BrdU incorporation pattern (Ito and Hotta, 1992) (Figure 2D). In the same batch of experiments, we found that 12 of 19 (63%), 16 of 28 (57%), or 11 of 38 (29%) of the larvae contained one *RhoA* MB Nb clone (i.e., two adjacent large nuclei in the MB region) when examined at 36, 18, or 16 hr after heat shock induction of mitotic recombination, respectively. Assuming the probability of inducing *RhoA* clone is independent of examination time, this experiment indicated that in the majority of the Nb clones, the last mitosis, which gave rise to the two large nuclei, had occurred by 18 hr after heat shock. Yet, BrdU incorporation still persisted at 18–24 hr after heat shock in 100% of the samples tested ($n = 18$; Figure 2C), indicating that there is at least one additional round of DNA replication after the last mitosis in the majority of *RhoA* Nb clones. This experiment argues against a G1/S block as the main cause of cell cycle arrest in *RhoA* Nb clones. *RhoA* Nb clones are also unlikely to arrest at the G2 stage, since no *RhoA* mutant cells contained detectable cyclin B staining (data not shown), a marker for G2 (Selleck et al., 1992; Knoblich and Lehner, 1993; Edgar et al., 1994).

To test whether there is a cytokinesis defect in *RhoA* Nb clones, we investigated the number of cell bodies

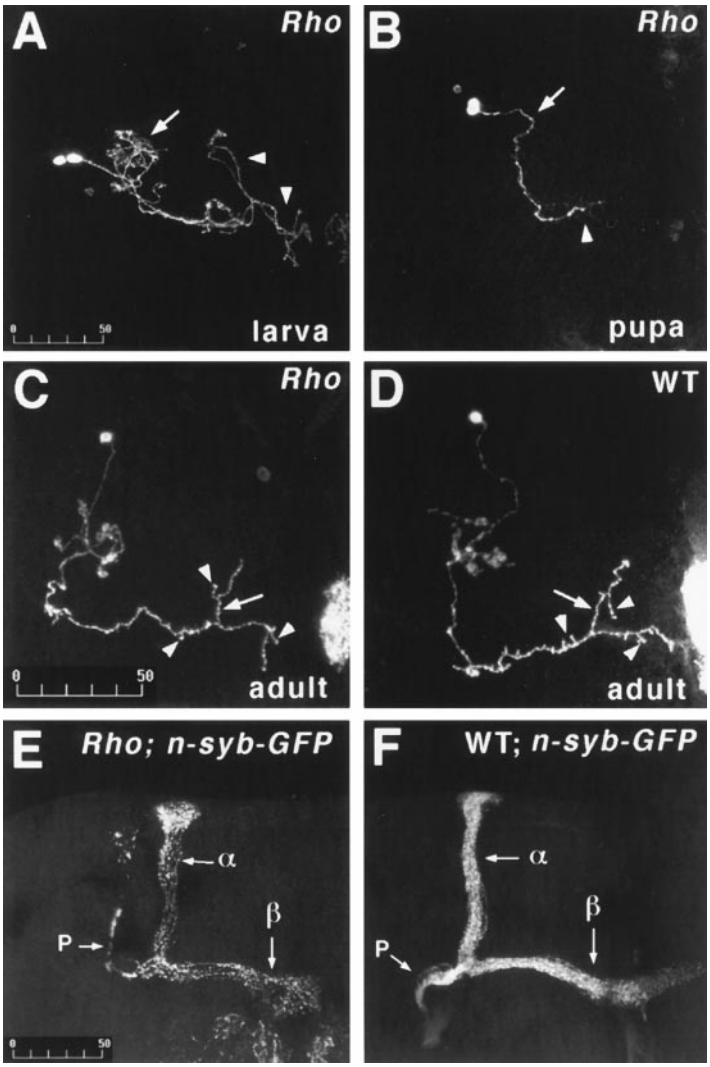


Figure 3. RhoA Is Not Required for Axonal Morphogenesis

(A–D) Two cell/single cell *RhoA* (A–C) or wild-type (D) MB clones, generated in newly hatched larvae, were examined in third instar larva (A) 18 hr after puparium formation (B) and in adults (C and D). *RhoA* neurons possess dendritic elaboration (arrow in [A]) and bifurcation of axons (arrowheads in [A]) at larval stage. These neurons degenerate their dendrites (arrow in [B]) and axonal branches in the lobes (arrowheads in [B]) at early pupal stage, as in wild type (Lee et al., 1999), and regenerate medial γ lobe–specific projections in adult (compare [C] and [D]). Within the γ lobe, branches longer than one quarter of the lobe length are defined as major branches (arrows in [C] and [D]), and all other branches are minor branches (arrowheads).

(E and F) MARCM clones of *RhoA* (E) and wild type (F) are visualized by *UAS-n-syb-GFP*, a synaptic vesicle marker. α and β lobes are labeled in these Nb clones since mitotic recombination was induced in pupal stage (Lee et al., 1999). Abbreviation: P, peduncle.

All images are composite confocal images. Genotypes: *hs-FLP/X* or *-Y*; $FRT^{G13}$,*UAS-mCD8-GFP*,$RhoA^{72O}$, *GAL4-201Y*/$FRT^{G13}$,*tubP-GAL80* (A–C); *hs-FLP/X* or *-Y*; $FRT^{G13}$,*UAS-mCD8-GFP*,*GAL4-201Y*/$FRT^{G13}$,*tubP-GAL80* (D); *GAL4-C155*,*hs-FLP/Y*; $FRT^{G13}$, $RhoA^{72R}$/$FRT^{G13}$,*tubP-GAL80*; *UAS-n-syb-GFP*/+ (E); and *GAL4-C155*,*hs-FLP/Y*; $FRT^{G13}$/$FRT^{G13}$, *tubP-GAL80*; *UAS-n-syb-GFP*/+ (F).

and nuclei in *RhoA* Nb clones. By double immunostaining for mCD8 and nuclear lamin, we demonstrated that mCD8-GFP, when expressed in neurons, is evenly distributed outside every nucleus and is a suitable marker for nuclear outlines (Figures 2E and 2F). Because a cytokinesis defect would predict the generation of multinucleated cells, we stained the plasma membrane specifically with anti-α-spectrin antibody (Prokopenko et al., 1999) and checked for any *RhoA* mutant cell body containing more than one nucleus (Figures 2G and 2H). We found that the two large *RhoA* mutant nuclei, the products of the last mitosis in *RhoA* Nb clones according to the BrdU labeling time course (Figures 2A–2D), were always present in the same cell body (n = 13; arrows in Figures 2G and 2H). In addition, one or two cell bodies were found to contain two small nuclei in each *RhoA* Nb clone (n = 13; arrowheads in Figures 2G and 2H). According to the cell proliferation pattern during neurogenesis (Figure 1A), two big nuclei in one cell body are probably due to a cytokinesis defect in a Nb, and two small nuclei in one cell body are likely derived from a ganglion mother cell with a cytokinesis defect. Therefore, this observation supports a cytokinesis defect as the main cause of cell division arrest in *RhoA* Nb clones. This result is consistent with the recent finding that the *Drosophila* Rho1/RhoA, as well as a putative exchange factor, Pebble, is essential for cytokinesis during embryogenesis (Prokopenko et al., 1999).

As revealed by the BrdU incorporation pattern (Figure 2C), DNA replication still persisted in Nbs arrested for cytokinesis. To estimate how extensively the DNA replication proceeded, we quantified the DNA content (see Experimental Procedures) and found that on average, each large nucleus possessed 3.30 ± 0.38-fold more DNA (mean ± SEM, n = 11) compared with a diploid nucleus. Taken together, these experiments indicate that in most proliferating *RhoA* Nbs, there was a slight endoreplication of DNA after the cytokinesis arrest. Interestingly, these multinuclear cells appear to acquire a differentiated neuronal fate based on the following criteria. The large nuclei-containing *RhoA* cells express a high level of *GAL4-C155*, which normally is expressed highly only in postmitotic neurons (Robinow and White, 1991; Lin and Goodman, 1994; Lee and Luo, 1999; Lee et al., 1999). They also express *GAL4-201Y*, which is not expressed in Nbs (T. L. et al., unpublished data; see

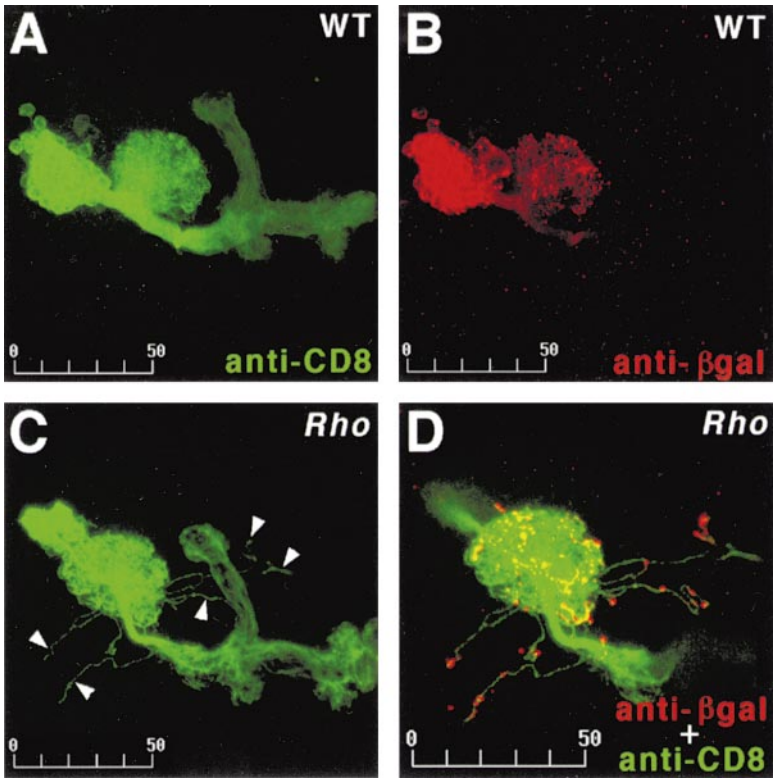


Figure 4. Dendritic Overextension in *RhoA* Mutant Neurons

(A and B) Coexpressing *mCD8-GFP* (A) and *Nod-β-gal* (B) in a wild-type Nb clone reveals preferential distribution of Nod-β-gal in cell bodies and dendrites.

(C) Fine processes (arrowheads) extend beyond the calyx region in a larval *RhoA* Nb clone.

(D) Close-up view of the calyx in (C) reveals concentration of Nod-β-gal (red) along and at the tips of overextending processes.

Genotypes: *GAL4-C155,hs-FLP/Y*; $FRT^{G13}$, *UAS-mCD8-GFP/*$FRT^{G13}$*,tubP-GAL80*; *UAS-Nod-β-gal/+* (A and B) and *GAL4-C155, hs-FLP/Y*; $FRT^{G13}$*,UAS-mCD8-GFP,*$RhoA^{72O}$/ $FRT^{G13}$, *tubP-GAL80; UAS-Nod-β-gal/+* (C and D).

below). In addition, neuronal processes that clearly projected from these cells were occasionally visible when Nb clones were less compact (see Figure 2E). Remarkably, these multinuclear cells live well into adulthood (Figure 1E).

**RhoA Is Not Required for Axonal Morphogenesis**

Rho has been implicated as an important regulator of the actin cytoskeleton and cell adhesion (Narumiya, 1996; Van Aelst and D'Souza-Schorey, 1997; Hall, 1998), processes that are crucial for axon growth and guidance. Surprisingly, neurons homozygous for *RhoA* null mutation project axons in a wild-type pattern (Figures 1C and 1E; see below). To examine axonal projections with high resolution, we analyzed single/two cell clones generated in newly hatched larvae to compare the fine details of wild-type and *RhoA* neurons that were born at the same time. Based on our previous birth-dating experiment (Lee et al., 1999), MB neurons born in the early larval stages are of the γ type, with axons projecting into the medial and dorsal lobes during larval stages. At the early pupal stage, these neurons completely degenerate their axon branches within the "larval" medial and dorsal lobes, then selectively reproject axons to the medial γ lobe (Lee et al., 1999). Throughout all stages, the *RhoA* axon projections were indistinguishable from those of wild type (Figures 3A–3D). To identify potential subtle changes, we quantified in single cell clones the number of major and minor branches within the adult γ lobe (see Figures 3C and 3D) and found no statistically significant differences between *RhoA* mutant and wild-type neurons. (Number of major branches: 1.9 ± 0.21 in wild type [n = 22] and 1.6 ± 0.20 in *RhoA* [n = 26], p = 0.22; number of minor branches: 10.3 ± 1.0 in wild type and 12.4 ± 0.82 in *RhoA*, p = 0.16. The numbers are mean ± SEM. p values were derived from two-tailed Student's t test.)

To assess a possible function of RhoA in synapse formation, we examined the distribution of n-syb-GFP, a synaptic vesicle marker constructed by fusing synaptobrevin with green fluorescent protein (GFP) (Ito et al., 1998). We found that wild-type and *RhoA* neurons exhibit a similar n-syb-GFP distribution, with the proteins highly concentrated in the peduncles and axonal lobes (Figures 3E and 3F).

*RhoA* mutant cells may inherit RhoA protein present in parental cells before mitotic recombination and hence may retain some RhoA activity. This could be why *RhoA* Nbs are able to divide a few times to give rise to 10–12 cells. However, the perdurance of RhoA activity is unlikely to explain the lack of an axonal phenotype. Even though residual parental RhoA protein may support larval axon projection, at the time of axonal degeneration and regeneration in the early pupal stage, mutant neurons have been deprived of the *RhoA* gene for 5 days. Moreover, the latest born *RhoA* neurons in Nb clones would inherit only highly diluted RhoA protein from a parental Nb that had divided 5–6 times without the *RhoA* gene. Yet, no axon defects were identified in either Nb or single/two cell clones, suggesting that RhoA is not necessary for correct axon outgrowth, guidance, degeneration, branch formation, or synaptic vesicle distribution.

**RhoA Is Essential in Limiting Dendrite Growth**

In contrast to the lack of axon defects, *RhoA* neurons showed a striking overextension of their dendrites. The

Table 1. Quantitative Analysis of Dendrite Overextension in Larval MB Nb Clones

| Genotype | Number of Cells per Clone | Total Number of Clones | Number of Clones with Over-extending Dendrites | Number of Clones with Long Over-extending Dendrites[d] | Average Number of Overextending Dendrites/Clone | |
|---|---|---|---|---|---|---|
| | | | | | Long | Short |
| Wild type[a] | ~100 | 37 | 13 (35.1%) | 3 (8.1%) | 0.08 | 0.41 |
| RhoA mutant[b] | 10–12 | 31 | 26 (83.9%) | 18 (58.1%) | 0.84 | 0.65 |
| RhoA$^{-}$+UAS-RhoA[c] | 10–12 | 27 | 3 (11.1%) | 2 (7.4%) | 0.07 | 0.04 |

Overextending dendrites were identified as Nod-LacZ-positive, green fluorescent processes protruding out of the calyx.
Genotypes:
[a] *hs-FLP/X* or *-Y; FRT$^{G13}$, UAS-mCD8-GFP,GAL4-201Y/FRT$^{G13}$, tubP-GAL80; UAS-Nod-β-gal/+*.
[b] *hs-FLP/X* or *-Y; FRT$^{G13}$, UAS-mCD8-GFP,RhoA$^{720}$,GAL4-201Y/FRT$^{G13}$,tubP-GAL80; UAS-Nod-β-gal/+*.
[c] *hs-FLP/X* or *-Y; FRT$^{G13}$,UAS-mCD8-GFP,RhoA$^{720}$,GAL4-201Y/FRT$^{G13}$,tubP-GAL80; UAS-Nod-β-gal,UAS-RhoA(WT)/+*.
[d] Long overextending dendrites were defined as processes protruding longer than one radius of the calyx.

10–12 *RhoA* mutant neurons in Nb clones projected extensive dendrites in wandering third instar larvae that appeared to occupy the entire calyx region (compare Figures 1B and 1C). Close examination revealed that *RhoA* neurons often projected their processes beyond the calyx region (Figure 4C). To determine whether the overextended processes from the calyx were dendrites, we tested the distribution of a fusion protein composed of the microtubule motor Nod and β-galactosidase (Nod-β-gal). Nod-β-gal has previously been shown to be concentrated at the tips of dendrites and largely absent from the axons of embryonic sensory neurons (Clark et al., 1997). We found that in wild-type MB neurons, Nod-β-gal was highly concentrated in the calyx and largely absent from peduncles and axon lobes in MB neurons (compare Figures 4A with 4B). In *RhoA* neurons, Nod-β-gal was also concentrated at the tips of all overextended processes (Figure 4D), thus identifying these processes as dendritic in nature. Occasionally, staining for Nod-β-gal distribution also revealed short overextension of dendrites in wild-type Nb clones. However, in *RhoA* clones, the length, frequency, and number of overextended dendrites were drastically increased compared with wild type (Table 1).

Single cell *RhoA* clones generated in newly hatched larvae rarely showed dendrite overextension (one overextending dendrite in 40 clones analyzed). This suggests that the overextended dendrites were largely contributed by later born neurons in *RhoA* mutant Nb clones, which presumably inherited less RhoA protein from parental cells. Indeed, *RhoA* Nb clones examined at 72 hr after larval hatching already exhibited significant dendrite overextension (data not shown), consistent with a requirement for RhoA activity to limit the extent of dendrite growth in an early stage of neuronal differentiation.

### Dendritic Growth Defect of *RhoA* Mutant Neurons Is Independent of the Nb Proliferation Defect

We have shown that RhoA is required for both Nb proliferation and limiting dendrite growth. The question arises whether they reflect separate functions of RhoA in regulating these processes, or whether it could be that one defect is a secondary consequence of another. To distinguish between these possibilities, we tried to rescue the dendritic phenotype specifically by expressing *UAS-RhoA(wt)* only in postmitotic neurons of *RhoA* mutant Nb clones. A MB GAL4 line, *GAL4-201Y* (Yang et al., 1995), was used in the following rescue experiment.

As expected, because *GAL4-201Y* cannot drive expression in Nbs, GAL4-201Y-controlled expression of *UAS-RhoA(wt)* in *RhoA* Nb clones (for genotype, see legend to Table 1) rescued the dendrite phenotype without affecting the proliferation defect. In the presence of the *UAS-RhoA(wt)* transgene, each mutant clone had 10–12 cells with two large nuclei (see Figure 1C; data not shown), while the frequency, number, and degree of dendrite overextension caused by *RhoA* mutation were restored to the wild-type level (Table 1). This experiment demonstrates that RhoA functions in postmitotic neurons to restrict dendritic extension and that the role of RhoA in the regulation of Nb proliferation and dendritic growth is likely to be independent.

### Cell-Autonomous Requirement for RhoA in Limiting Dendrite Growth

Because RhoA is an intracellular signaling protein, it is generally assumed that it would exert its function through a cell-autonomous mechanism. Because single neurons homozygous for *RhoA* failed to show significant phenotype (see above), we cannot conclude that RhoA is cell autonomously required to limit dendritic growth, even if RhoA is only deficient in labeled groups of MB neurons. It is possible that lack of RhoA in neuron 1 signals to a neighboring neuron 2 to overextend its dendrite, regardless of the genotype of neuron 2.

To test rigorously whether RhoA functions in a cell-autonomous fashion, we employed a "reverse-MARCM" strategy (Figure 5A). The *RhoA* null mutation was placed on the same chromosome arm as the *tubP-GAL80* transgene, such that the homozygous *RhoA* mutant cells will not be labeled; instead, the sibling from the mitotic recombination, which is homozygous wild type for *RhoA*, will be selectively labeled. Given the cell division pattern (Figure 1A), if we observe a labeled two cell (wild-type) clone, we can infer that an unlabeled *RhoA* Nb clone must have been generated concurrently. Therefore, the labeled wild-type cells (as a two cell clone) should be in closest contact with a *RhoA* mutant Nb clone (for example, see Figures 5D and 5E). If there were a non cell-autonomous effect of RhoA in regulating dendrite growth, these two labeled cells would be the nonmutant cells most likely to exhibit a dendritic overextension phenotype.

As shown in Figures 5B and 5C, the two cell clones of wild-type neurons elaborate their dendrites within the confines of the MB calyx, which was independently

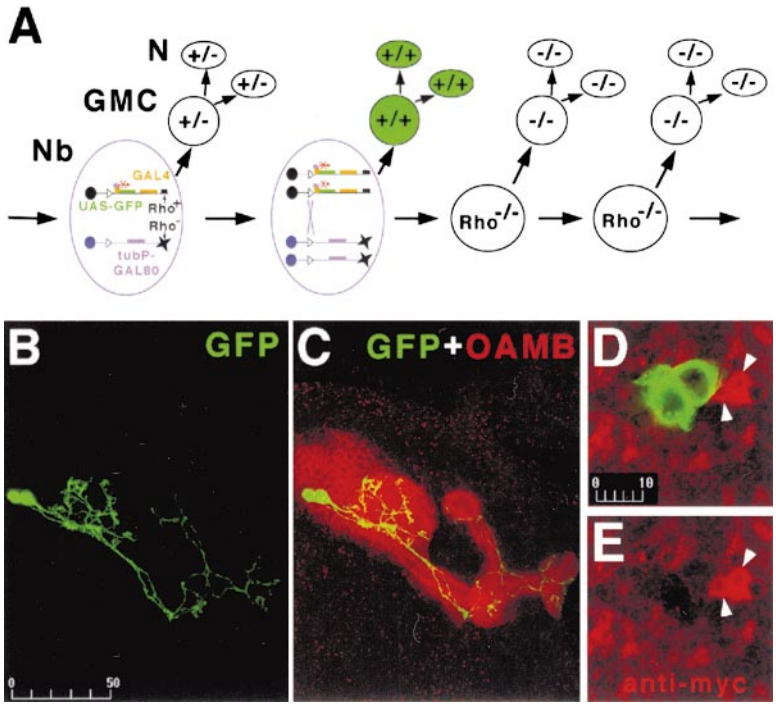


Figure 5. Cell-Autonomous Function of RhoA in Limiting Dendrite Growth, as Revealed by a Reverse MARCM Strategy

(A) In the reverse MARCM strategy, the mutant allele (*RhoA*) is on the same chromosome arm as is the *tubP-GAL80* transgene, so the homozygous wild-type clone, rather than the mutant clone, becomes marked after a mitotic recombination. A labeled homozygous wild-type two cell clone is therefore always coupled with an invisible, homozygous mutant Nb clone. Note that the first Nb in the schematic drawing is shown at the G1 stage, and the second Nb is shown at the G2 stage after DNA replication. Abbreviations: Nb, neuroblast; GMC, ganglion mother cell; and N, neurons.

(B and C) Composite confocal images of a GFP-positive wild-type two cell MB clone, which was generated in conjunction with an invisible *RhoA* mutant Nb clone using the reverse MARCM strategy. In (C), the whole MB was visualized by staining with anti-OAMB antibody (red). Note that the GFP-positive dendrites are within the calyx region.

(D and E) Simultaneous labeling of mosaic tissues with the MARCM (green) and negative-labeling (red) systems (Xu and Rubin, 1993). The *RhoA* Nb clone was marked as GFP-positive and Myc-negative cells, while the two cell wild-type clone, derived from the same mitotic recombination, appeared as strong Myc-positive cells. In all cases, when Myc staining is clear, we can identify two strong Myc-positive cells (arrowheads) adjacent to the large Myc-negative, GFP-positive nuclei of *RhoA* Nb clones.

Genotypes: *hs-FLP/X* or *-Y*; $FRT^{G13}$,*UAS-mCD8-GFP*, *GAL4-201Y*/$FRT^{G13}$,*tubP-GAL80*,$RhoA^{72R}$ (B and C) and *hs-FLP/X*; $FRT^{G13}$,*UAS-mCD8-GFP*,$RhoA^{72O}$, *GAL4-201Y*/$FRT^{G13}$,*tubP-GAL80*,*hs-πMyc* (D and E).

labeled by immunofluorescence using anti-OAMB against an octopamine receptor preferentially expressed in the MBs (Han et al., 1998) (red in Figure 5C). We have examined a total of 34 clones and have not observed any overextending dendrites. Using the standard MARCM assay, in which only the mutant cells are labeled, we calculated that >10% of the labeled neurons (on average, 1.48 overextending dendrites from a 10 cell clone) exhibited dendrite overgrowth (Table 1). If RhoA acts non cell autonomously, we would expect a similar percentage of labeled neurons producing overextended dendrites under reverse-MARCM conditions. The fact that we do not observe a single overextended dendrite in 68 neurons examined indicates that RhoA acts cell autonomously to regulate dendrite growth.

### Constitutively Active RhoA Expression Results in a Reduction of Dendritic Volume and Density

Since loss of RhoA activity resulted in dendritic overextension, we tested whether elevation of RhoA activity would cause an opposite phenotype under two experimental conditions. First, we expressed a constitutively active form of RhoA(V14) in MB neurons via the GAL4-UAS system (Brand and Perrimon, 1993) using *GAL4-201Y* (Yang et al., 1995; see above). We found a 50% reduction of the volume of dendritic field in RhoA(V14)-expressing MBs compared with control (Figures 6A–6C), whereas no abnormality in axonal projections was detectable (Figures 6A and 6B). In contrast, analogous expression of constitutively active Rac1(V12) or Cdc42(V12) in MB neurons resulted in drastic defects in axon growth and guidance (T. L. et al., unpublished data). Second, we expressed RhoA(V14) in only one MB clone using the MARCM strategy. Interestingly, while the dendritic field volume appears unaffected, there is a 50% reduction of dendritic density (Figures 6D and 6E), as measured by relative fluorescence intensity of the calyx (Figure 6F).

In both experiments, the transgene is only expressed in postmitotic MB neurons using *GAL4-201Y*, so an effect on Nb proliferation is unlikely. Indeed, there is no change in the total number of MB neurons in either experiment (see legend to Figures 6C and 6F). Moreover, these neurons are positive for the MB *GAL4-201Y* line, and they have MB-specific axonal and dendritic projection, which argues against the possibility that their fates are changed. Therefore, we think that RhoA(V14) most likely affects dendritic morphogenesis directly.

One possible explanation for the differential effects seen in the two experiments is how many MB neurons are affected. There are four MB Nbs on each side of the brain, and each Nb contributes to a set of similar, if not identical, MB neurons (Ito et al., 1997; Lee and Luo, 1999). When RhoA(V14) is expressed in all early born neurons using *GAL4-201Y*, all dendrites are affected in the same way, and hence, the net outcome is a reduction of the entire dendritic field volume. In contrast, when RhoA(V14) is expressed only in a clone of MB neurons via the MARCM strategy, the mutant dendrites can extend to the larger dendritic field created by wild-type dendrites from MB neurons derived from the other three MB Nbs. The predominant effect is then a reduction in dendritic density, a manifestation consistent with a decrease of length or branching complexity of dendrites

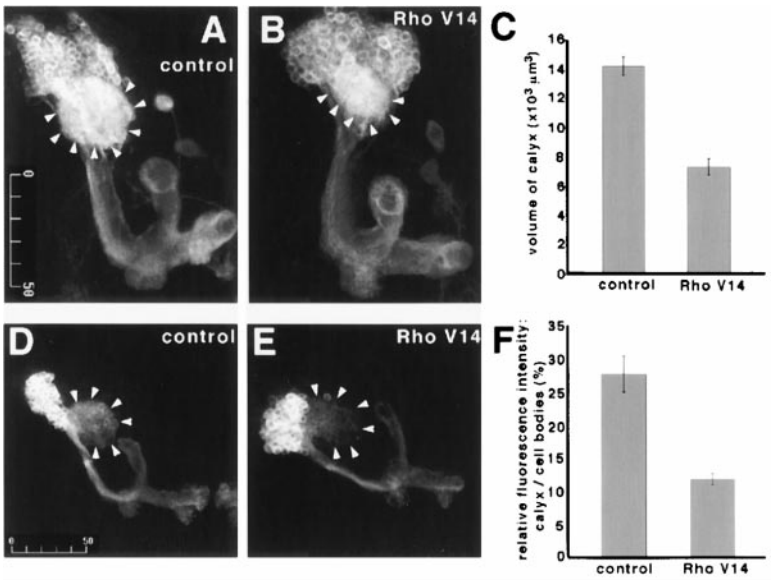


Figure 6. Reduction in the Calyx Volume and Density of Constitutively Active RhoA(V14)-Expressing MB Neurons

(A and B) Composite confocal images of whole MBs expressing mCD8-GFP alone (A) or mCD8-GFP plus RhoA(V14) (B) driven by *GAL4-201Y*. Note that the calyx size is much reduced in the *RhoA(V14)* MB. Calyces are outlined by arrows.

(C) Quantification of calyx volumes. The volume was calculated as the sum of calyx areas on individual planes (measured with the Laser Sharp program) multiplied by the Z step (1 μm). Error bars represent SEM; $n = 10$, $p < 10^{-7}$ according to one-tailed Student's t test. There is no significant difference in the volume of cell body region between the two genotypes ($p = 0.45$).

(D and E) Composite confocal images of MB Nb clones expressing mCD8-GFP alone (D) or mCD8-GFP plus RhoA(V14) (E). Note that the calyx of the *RhoA(V14)* clone looks much less dense.

(F) Quantification of relative calyx densities. For each clone, the intensities of fluorescence signals of both cell body and calyx regions were measured using the NIH Image program. The relative calyx density was then calculated as the ratio of fluorescence intensity of calyx over cell bodies. Error bars represent SEM; $n = 10$, $p < 10^{-4}$ according to one-tailed Student's t test. There is no significant difference in the number of cell bodies between the two genotypes ($p = 0.08$).

Genotypes: *UAS-mCD8-GFP,GAL4-201Y/+* (A); *UAS-mCD8-GFP,GAL4-201Y/+*; *UAS-RhoA(V14)/+* (B); *hs-FLP/X* or *-Y*; *FRT$^{G13}$,UAS-mCD8-GFP*, *GAL4-201Y/FRT$^{G13}$,tubP-GAL80* (D); and *hs-FLP/X* or *-Y*; *FRT$^{G13}$,UAS-mCD8-GFP,GAL4-201Y/FRT$^{G13}$, tubP-GAL80*; *UAS-RhoA(V14)/+* (E).

from individual RhoA(V14)-expressing neurons. Both experiments suggest that the expression of activated RhoA resulted in phenotypes opposite to that of loss-of-function mutant: the reduction in size or density of the dendritic field compared with the overextension of dendrites.

### Mechanistic Implications of Differential Effects of RhoA on the Morphogenesis of Axons and Dendrites

Previous cell culture studies suggested that RhoA mediates cell rounding and neurite retraction in response to extracellular agonists. For instance, inhibition of RhoA via C3 exoenzyme ribosylation inhibited agonist-induced cell rounding and process retraction (Jalink et al., 1994; Kozma et al., 1997; Hirose et al., 1998), whereas expression of activated RhoA(V14) resulted in agonist-independent process retraction and growth cone collapse (Kozma et al., 1997). RhoA inhibition was further shown to block the generation of actomyosin-based contractile forces likely to be responsible for process retraction (Jalink et al., 1994). Indeed, one specific effector pathway, the regulation of myosin light chain phosphorylation via the activation of Rho-associated kinase (ROCK), was shown to mediate RhoA-induced neurite retraction (Hirose et al., 1998). In cultured neuronal-like cells, however, there is no morphological differentiation of axons and dendrites. Here, we demonstrate that RhoA is cell autonomously required to limit dendritic growth of CNS neurons in vivo. Our analyses also strongly suggest that RhoA is not essential for growth, guidance, degeneration, and regeneration of the axons of MB neurons. These findings are further supported by the fact that constitutively active RhoA expression results in a reduction of dendritic volume and density without detectable effects on axons. In a separate study, we showed that activation of RhoA in mammalian hippocampal pyramidal neurons in slice culture resulted in a drastic simplification of dendritic complexity and that ROCK is essential in mediating this effect (A. Y. Nakayama et al., submitted). These studies demonstrate an evolutionarily conserved role for the GTPase RhoA in negatively regulating dendritic growth, probably via the regulation of actomyosin-based contractility.

What are the likely explanations for the preferential requirement of RhoA in dendritic but not axonal morphogenesis? One possibility is that in clonal analyses described in this study, axons from *RhoA* neurons are not pioneer axons. *RhoA* axons may adhere to and follow the path of wild-type MB axons derived from neurons either generated from the same Nb before the clone was generated or from three other wild-type MB Nbs (Ito et al., 1997; Lee et al., 1999). In contrast to axons, lack of fasciculation of dendritic processes and their highly diverse branching patterns (see Figures 3A and 5B) suggest that dendritic growth and elaboration from individual neurons may be more independent of one another. It remains possible that *RhoA* is required for the growth and guidance of pioneering axons, which may have different molecular requirements (e.g., see Hedgecock et al., 1990). However, the growth and guidance of such nonpioneering axons are disrupted when *short stop* is mutated (Lee and Luo, 1999). Another possible explanation is that the "stop signals" for dendritic growth are sent from the termini of incoming axons, and RhoA is an essential component of such a signal transduction pathway. The signal transduction pathway at the axonal growth cone for stopping growth may be distinct from those within the dendritic equivalent. The differential requirement of RhoA in the morphogenesis of axons

and dendrites may also reflect the inherent differences in these two neuronal compartments in their cytoskeletal polarity and process growth rate (reviewed by Craig and Banker, 1994). For instance, a recent study of cultured hippocampal neurons revealed differential stability of the actin cytoskeleton in the growth cones of axons and dendrites. By destabilizing actin cytoskeleton through pharmacological agents or inhibitors of Rho GTPases, processes that would otherwise develop into dendrites can be converted into longer, axon-like processes (Bradke and Dotti, 1999). In our study, inhibition of RhoA also resulted in abnormal long processes. However, we demonstrated that these neuronal processes are dendritic in nature, judging from both their location and the distribution of Nod-β-gal. Whatever the detailed mechanisms are, this study underscores the differences in the molecular requirements of axon and dendrite morphogenesis, a conclusion also supported by our previous studies of another small GTPase, Rac1 (Luo et al., 1994, 1996). Interestingly, in both sensory neurons of *Drosophila* embryos (Luo et al., 1994) and mouse Purkinje cells (Luo et al., 1996), expression of dominant mutants of Rac1 resulted in preferential inhibition of axonal growth. Taken together, these observations suggest that different Rho family GTPases preferentially regulate the morphogenesis of different neuronal compartments.

The last few years have witnessed enormous progress in our understanding of the molecular mechanisms of axon growth and guidance (reviewed by Goodman, 1996; Mueller, 1999; Song and Poo, 1999). While a genetic screen for mutants affecting dendrite morphogenesis of *Drosophila* embryonic sensory neurons has recently been described (Gao et al., 1999), much less is known about the mechanisms involved in the elaboration of dendrites, largely because of their morphological complexity. The ability to visualize and genetically manipulate a small population of neurons and their dendrites allowed for analysis of their morphology in greater detail and has led to the identification of RhoA as an important regulator of dendritic growth. Further investigation of the RhoA signaling pathway and the identification of other molecules and pathways using analogous genetic mosaic approaches will shed more light on the molecular mechanisms controlling dendrite morphogenesis.

## Experimental Procedures

### Fly Strains

Standard genetic methods were used to generate the following 17 fly stocks: (1–2) *FRT$^{G13}$,UAS-mCD8-GFP,RhoA$^{72O/72R}$/CyO*; (3–4) *FRT$^{G13}$,UAS-mCD8-GFP,RhoA$^{72O/72R}$/CyO*; *UAS-RhoA*; (5–6) *FRT$^{G13}$, UAS-mCD8-GFP,RhoA$^{72O/72R}$,GAL4-201Y/CyO*; (7) *FRT$^{G13}$*; *UAS-n-syb-GFP*; (8) *FRT$^{G13}$,RhoA$^{72R}$/CyO*; *UAS-n-syb-GFP*; (9) *FRT$^{G13}$,UAS-mCD8-GFP*; *UAS-Nod-β-gal*; (10) *FRT$^{G13}$,UAS-mCD8-GFP,RhoA$^{72O}$/CyO*; *UAS-Nod-β-gal*; (11) *FRT$^{G13}$,UAS-mCD8-GFP,GAL4-201Y*; *UAS-Nod-β-gal*; (12) *FRT$^{G13}$,UAS-mCD8-GFP,RhoA$^{72O}$,GAL4-201Y/CyO*; *UAS-Nod-β-gal*; (13) *FRT$^{G13}$,UAS-mCD8-GFP,RhoA$^{72O}$, GAL4-201Y/CyO*; *UAS-Nod-β-gal,UAS-RhoA*; (14) *hs-FLP; FRT$^{G13}$, UAS-mCD8-GFP,GAL4-201Y*; (15) *FRT$^{G13}$,tubP-GAL80,RhoA$^{72R}$/CyO*; (16) *FRT$^{G13}$,tubP-GAL80*; *UAS-RhoA(V14)*; and (17) *hs-FLP*; *FRT$^{G13}$,tubP-GAL80,hs-πMyc*. All other stocks used were reported earlier (Lee and Luo, 1999; Lee et al., 1999).

### Generation and Visualization of MARCM Clones

Larvae (0–2 hr; for genotypes, see figure legends) were collected and placed on standard fly food at a density of 80 larvae/vial. A 40 min heat shock at 37°C was applied immediately (except in Figures 3E and 3F, where heat shock was performed at the pupal stage) to induce the expression of the *hs-FLP* transgene, and hence mitotic recombination. Because MB Nbs are the predominant Nbs undergoing active proliferation in newly hatched larvae, MB clones are highly enriched under this experimental condition (Lee and Luo, 1999). At desired stages, brains were dissected, fixed, and immunostained as previously described (Lee and Luo, 1999). For induction of *hs-πMyc* to visualize the twin spot (Figures 5D and 5E), organisms were additionally heat shocked at 37°C for 1 hr and then dissected 1 hr later. Neurons were mostly visualized with a membrane marker, mCD8-GFP (Lee and Luo, 1999). Primary antibody dilutions: anti-mCD8 (rat monoclonal antibody (mAb), Caltag), 1:100; anti-lamin (rabbit antibody from P. Fisher), 1:50; anti-BrdU (mouse mAb, Roche), 1:20; anti-β-gal (rabbit antibody, Cappel), 1:10,000; anti-cyclin B (mouse mAb developed by P. O'Farrell and obtained from the Developmental Studies Hybridoma Bank, supported by the National Institute of Child Health and Development and the University of Iowa), 1:20; anti-OAMB (Han et al., 1998), 1:100; anti-α-spectrin (antibody 354; Byers et al., 1987), 1:300; and anti-Myc (mouse mAb, Santa Cruz), 1:50. For double labeling involving anti-mCD8, FITC-conjugated secondary antibody was used for detecting mCD8-GFP, and Cy3-conjugated secondary antibody was used to detect the other antigen.

### BrdU Incorporation

For BrdU incorporation experiments, BrdU was added to food at a concentration of 0.75 mg/ml. A 30 min incubation in 2 N HCl (in phosphate-buffered saline [PBS]) was included before anti-BrdU staining.

### Quantification of DNA Content

Newly hatched larvae (for genotype, see Figure 2 legend) were heat shocked and grown on regular fly food for 36 hr. CNSs were dissected in cold PBS and transferred to poly-lysine-coated slides for squashing into a monolayer of cells. Subsequent preparation and 4′,6-diamidino-2-phenylindole (DAPI) staining of the tissue were performed as described (Smith and Orr-Weaver, 1991). Large *RhoA* cell bodies were identified by GFP fluorescence. DAPI fluorescence of large *RhoA* cells and neighboring postmitotic neurons were collected using a cooled charge-coupled device camera and quantified using the MetaMorph program. The relative DNA content for each large cell was normalized against the average of six randomly chosen normal cells in the same slide after correction of area-based background.

### Acknowledgments

We thank M. Mlodzik for *RhoA* mutants and *UAS-RhoA* transgenic flies; I. Clark and Y. N. Jan for *UAS-Nod-β-gal* flies; M. Ramaswami for *UAS-n-syb-GFP* flies; P. Fisher for the anti-lamin antibody; K. A. Han and R. Davis for the anti-OAMB antibody; D. Branton for the anti-α-spectrin antibody; R. Kopito for the use of imaging setup; B. Baker, J. Knoblich, S. McConnell, P. O'Farrell, M. Scott, M. Simon, the anonymous reviewers, and members of the Luo lab for discussions and comments on the manuscript. T. L. and C. W. are recipients of National Research Service Award fellowships from the National Institutes of Health. This work was supported by grants from the National Institutes of Health (R01-NS36623) and the Muscular Dystrophy Association to L. L., who is a Klingenstein, McKnight, and Sloan fellow or scholar.

Received November 9, 1999; revised December 9, 1999.

### References

Barrett, K., Leptin, M., and Settleman, J. (1997). The Rho GTPase and a putative RhoGEF mediate a signaling pathway for the cell shape changes in Drosophila gastrulation. Cell *91*, 905–915.

Bradke, F., and Dotti, C.G. (1999). The role of local actin instability in axon formation. Science *283*, 1931–1934.

Brand, A.H., and Perrimon, N. (1993). Targeted gene expression as a means of altering cell fates and generating dominant phenotypes. Development *118*, 401–415.

Byers, T.J., Dubreuil, R., Branton, D., Kiehart, D.P., and Goldstein, L.S. (1987). *Drosophila* spectrin. II. Conserved features of the alpha-subunit are revealed by analysis of cDNA clones and fusion proteins. J. Cell Biol. *105*, 2103–2110.

Clark, I.E., Jan, L.Y., and Jan, Y.N. (1997). Reciprocal localization of Nod and kinesin fusion proteins indicates microtubule polarity in the *Drosophila* oocyte, epithelium, neuron and muscle. Development *124*, 461–470.

Craig, A.M., and Banker, G. (1994). Neuronal polarity. Annu. Rev. Neurosci. *17*, 267–310.

Crittenden, J.R., Sloulakis, E.M.C., Han, K.-A., Kalderon, D., and Davis, R.L. (1998). Tripartite mushroom body architecture revealed by antigenic markers. Learn Mem. *5*, 38–51.

Edgar, B.A., Sprenger, F., Duronio, R.J., Leopold, P., and O'Farrell, P.H. (1994). Distinct molecular mechanism regulate cell cycle timing at successive stages of *Drosophila* embryogenesis. Genes Dev. *8*, 440–452.

Gao, F.B., Brenman, J.E., Jan, L.Y., and Jan, Y.N. (1999). Genes regulating dendritic outgrowth, branching, and routing in *Drosophila*. Genes Dev. *13*, 2549–2561.

Goodman, C.S. (1996). Mechanisms and molecules that control growth cone guidance. Annu. Rev. Neurosci. *19*, 341–377.

Hall, A. (1998). Rho GTPases and the actin cytoskeleton. Science *279*, 509–514.

Han, K.A., Millar, N.S., and Davis, R.L. (1998). A novel octopamine receptor with preferential expression in *Drosophila* mushroom bodies. J. Neurosci. *18*, 3650–3658.

Hariharan, I.K., Hu, K.Q., Asha, H., Quintanilla, A., Ezzell, R.M., and Settleman, J. (1995). Characterization of rho GTPase family homologues in *Drosophila melanogaster*: overexpressing Rho1 in retinal cells causes a late developmental defect. EMBO J. *14*, 292–302.

Hedgecock, E.M., Culotti, J.G., and Hall, D.H. (1990). The unc-5, unc-6, and unc-40 genes guide circumferential migrations of pioneer axons and mesodermal cells on the epidermis in C. elegans. Neuron *4*, 61–85.

Hirose, M., Ishizaki, T., Watanabe, N., Uehata, M., Kranenburg, O., Moolenaar, W.H., Matsumura, F., Maekawa, M., Bito, H., and Narumiya, S. (1998). Molecular dissection of the Rho-associated protein kinase (p160ROCK)-regulated neurite remodeling in neuroblastoma N1E-115 cells. J. Cell Biol. *141*, 1625–1636.

Ito, K., and Hotta, Y. (1992). Proliferation pattern of postembryonic neuroblasts in the brain of *Drosophila melanogaster*. Dev. Biol. *149*, 134–148.

Ito, K., Awano, W., Suzuki, K., Hiromi, Y., and Yamamoto, D. (1997). The *Drosophila* mushroom body is a quadruple structure of clonal units each of which contains a virtually identical set of neurons and glial cells. Development *124*, 761–771.

Ito, K., Suzuki, K., Estes, P., Ramaswami, M., Yamamoto, D., and Strausfeld, N.J. (1998). The organization of extrinsic neurons and their implications in the functional roles of the mushroom bodies in *Drosophila melanogaster* meigen. Learn. Mem. *5*, 52–77.

Jalink, K., van Corven, E.J., Hengeveld, T., Morii, N., Narumiya, S., and Moolenaar, W.H. (1994). Inhibition of lysophosphatidate- and thrombin-induced neurite retraction and neuronal cell rounding by ADP ribosylation of the small GTP-binding protein Rho. J. Cell Biol. *126*, 801–810.

Kishi, K., Sasaki, T., Kuroda, S., Itoh, T., and Takai, Y. (1993). Regulation of cytoplasmic division of *Xenopus* embryo by rho p21 and its inhibitory GDP/GTP exchange protein (rhoGDI). J. Cell Biol. *120*, 1187–1195.

Knoblich, J.A., and Lehner, C.F. (1993). Synergistic action of *Drosophila* cyclins A and B during the G2-M transition. EMBO J. *12*, 65–74.

Kozma, R., Sarner, S., Ahmed, S., and Lim, L. (1997). Rho family GTPases and neuronal growth cone remodelling: relationships between increased complexity induced by Cdc42Hs, Rac1, and acetylcholine and collapse induced by RhoA and lysophosphatidic acid. Mol. Cell. Biol. *17*, 1201–1211.

Lee, T., and Luo, L. (1999). Mosaic analysis with a repressible cell marker for studies of gene function in neuronal morphogenesis. Neuron *22*, 451–461.

Lee, T., Lee, A., and Luo, L. (1999). Development of the *Drosophila* mushroom bodies: sequential generation of three distinct types of neurons from a neuroblast. Development *126*, 4065–4076.

Lin, D.M., and Goodman, C.S. (1994). Ectopic and increased expression of Fasciclin II alters motoneuron growth cone guidance. Neuron *13*, 507–523.

Lu, Y., and Settleman, J. (1999). The *Drosophila* Pkn protein kinase is a Rho/Rac effector target required for dorsal closure during embryogenesis. Genes Dev. *13*, 1168–1180.

Luo, L., Liao, Y.J., Jan, L.Y., and Jan, Y.N. (1994). Distinct morphogenetic functions of similar small GTPases: *Drosophila* Drac1 is involved in axonal outgrowth and myoblast fusion. Genes Dev. *8*, 1787–1802.

Luo, L., Hensch, T.K., Ackerman, L., Barbel, S., Jan, L.Y., and Jan, Y.N. (1996). Differential effects of the Rac GTPase on Purkinje cell axons and dendritic trunks and spines. Nature *379*, 837–840.

Luo, L., Jan, L.Y., and Jan, Y.N. (1997). Rho family small GTP-binding proteins in growth cone signaling. Curr. Opin. Neurobiol. *7*, 81–86.

Mabuchi, I., Hamaguchi, Y., Fujimoto, H., Morii, N., Mishima, M., and Narumiya, S. (1993). A rho-like protein is involved in the organization of the contractile ring in dividing sand dollar eggs. Zygote *1*, 325–331.

Mueller, B.K. (1999). Growth cone guidance: first steps towards a deeper understanding. Annu. Rev. Neurosci. *22*, 351–388.

Narumiya, S. (1996). The small GTPase Rho: cellular functions and signal transductions. J. Biochem. *120*, 215–228.

Olson, M.F., Ashworth, A., and Hall, A. (1995). An essential role for Rho, Rac, and Cdc42 GTPases in cell cycle progression through G1. Science *269*, 1270–1272.

Prokopenko, S.N., Brumby, A., O'Keefe, L., Prior, L., He, Y., Saint, R., and Bellen, H.J. (1999). A putative exchange factor for Rho1 GTPase is required for initiation of cytokinesis in *Drosophila*. Genes Dev. *13*, 2301–2314.

Robinow, S., and White, K. (1991). Characterization and spatial distribution of the ELAV protein during *Drosophila melanogaster* development. J. Neurobiol. *22*, 443–461.

Selleck, S.B., Gonzalez, C., Glover, D.M., and White, K. (1992). Regulation of the G1-S transition in postembryonic neuronal precursors by axon ingrowth. Nature *355*, 253–255.

Smith, A.V., and Orr-Weaver, T.L. (1991). The regulation of the cell cycle during *Drosophila* embryogenesis: the transition to polyteny. Development *112*, 997–1008.

Smith, D.E., and Fisher, P.A. (1989). Interconversion of *Drosophila* nuclear lamin isoforms during oogenesis, early embryogenesis, and upon entry of cultured cells into mitosis. J. Cell Biol. *108*, 255–265.

Song, H.-j., and Poo, M.-m. (1999). Signal transduction underlying growth cone guidance by diffusible factors. Curr. Opin. Neurobiol. *9*, 355–363.

Strutt, D.I., Weber, U., and Mlodzik, M. (1997). The role of RhoA is tissue polarity and Frizzled signaling. Nature *387*, 292–295.

Threadgill, R., Bobb, K., and Ghosh, A. (1997). Regulation of dendritic growth and remodeling by Rho, Rac, and Cdc42. Neuron *19*, 625–634.

Valencia, A., Chardin, P., Wittinghofer, A., and Sander, C. (1991). The *ras* protein family: evolutionary tree and role of conserved amino acids. Biochemistry *30*, 4637–4648.

Van Aelst, L., and D'Souza-Schorey, C. (1997). Rho GTPases and signaling networks. Genes Dev. *11*, 2295–2322.

Xu, T., and Rubin, G.M. (1993). Analysis of genetic mosaics in developing and adult Drosophila tissues. Development *117*, 1223–1237.

Yamamoto, M., Marui, N., Sakai, T., Morii, N., Kozaki, S., Ikai, K., Imamura, S., and Narumiya, S. (1993). ADP-ribosylation of the rhoA gene product by botulinum C3 exoenzyme causes Swiss 3T3 cells to accumulate in the G1 phase of cell cycle. Oncogene *8*, 1449–1455.

Yang, M.Y., Armstrong, J.D., Vilinsky, I., Strausfeld, N.J., and Kaiser, K. (1995). Subdivision of the Drosophila mushroom bodies by enhancer-trap expression pattern. Neuron *15*, 45–54.